HHS Public Access

Author manuscript

Dent Mater. Author manuscript; available in PMC 2021 November 01.

Published in final edited form as:

Dent Mater. 2020 November ; 36(11): 1407–1417. doi:10.1016/j.dental.2020.08.015.

Wear behavior and microstructural characterization of translucent multilayer zirconia

Sonaj Vardhaman[a], **Marcia Borba**[a,b], **Marina R. Kaizer**[a,c], **DoKyung Kim**[a,d], **Yu Zhang**[a,*]

[a]Department of Biomaterials and Biomimetics, New York University College of Dentistry, USA.

[b]Post-graduate Program in Dentistry, University of Passo Fundo, Brazil.

[c]Post-graduate Program in Dentistry, Positivo University, Brazil.

[d]Department of Materials Science and Engineering, KAIST, South Korea.

Abstract

Objective.—To characterize the composition, microstructure and wear properties of a multilayer translucent zirconia relative to the conventional 3Y-TZP.

Methods.—Two types of ceramics were evaluated: a multilayer zirconia (MULTI, IPS e.max ZirCAD Multi, Ivoclar Vivadent) and a control 3Y-TZP (IPS e.max ZirCAD LT, Ivoclar Vivadent). Pre-sintered CAD-CAM blocks were cut, ground, sintered and polished to 1 μm finish. The phase fraction and grain size were measured using XRD and FE-SEM. For wear testing (n = 12), square-shaped specimens (16x16x1 mm) were adhesively bonded to a dentin analog. Sliding wear tests were performed using a spherical zirconia antagonist (r = 3.15 mm), with 30 N load at 1.5 Hz for 500,000 cycles in water. Optical and scanning electron microscopes and 3D laser scanner were used for quantitative wear analyses. Data were analyzed using Student´s t-test (α = 0.05).

Results.—For MULTI, the enamel layer had the highest cubic content and the largest grain size, followed by the two transition layers, and the dentin layer. 3Y-TZP showed the smallest grain size and cubic content. A significant amount of wear was observed in both materials up to 50,000 cycles until it reached a plateau. MULTI showed higher volume loss and greater wear depth than 3Y-TZP ($p < 0.01$). The higher volume loss was associated with extensive lateral fracture, leading to material spalling from the surface of cubic-containing zirconias.

Significance.—The wear pattern in multi-layered zirconia was more severe than 3Y-TZP. Additionally, the different layers of the multi-layered zirconia had similar wear behavior.

Keywords

ceramics; prostheses; occlusion; sliding contact; wear parameters; wear mechanisms

*Corresponding author: Prof. Yu Zhang, Department of Biomaterials and Biomimetics, New York University College of Dentistry, 433 First Avenue, Room 810, New York, NY 10010, USA, Tel.: +1 212 998 9637.

Declaration

The authors declare that there is no conflict of interest.

1. Introduction

Dental materials must combine good physical and mechanical properties with tooth-like esthetics in order to provide restorative treatments with high survival rates and to guarantee the patient´s satisfaction. The composition and microstructure of the first-generation zirconia, specifically 3 mol.% yttria stabilized tetragonal zirconia polycrystals (3Y-TZP), were tailored to optimize its strength and toughness rather than translucency. Thus, they are suitable for the frameworks of crowns and bridges, as well as implants and abutments [1]. The improved translucency in the second-generation zirconia was achieved by reducing the content of alumina sintering additives while increasing its bulk density [2, 3]. Such an effort ultimately expanded the clinical indication of zirconia to monolithic posterior crowns and bridges [3-5]. Further improvement of translucency of the third-generation zirconia was realized by increasing the quantity of yttria stabilizer, leading to higher amounts of optically isotropic cubic phase content [3, 4]. The tradeoff is that these highly translucent, cubic-containing zirconias also exhibited lower strength and toughness relative to the first and second generations of 3Y-TZP [3-6]. Therefore, they are clinically indicated for veneers, inlays, onlays, crowns, and anterior bridges up to 3 units [4, 5].

Despite much improved translucency, the first 3 generations of zirconia are monochrome. In order to produce a restoration with a more natural appearance, the fourth-generation, multichromatic zirconia with a layered structure have been developed to mimic the shade and translucency gradients found in natural teeth [5, 7]. In that first multilayer zirconia system introduced to restorative dentistry (Katana, Kuraray Noritake), the same yttrium content and cubic fraction were observed in the different layers of the materials. The only difference among those layers was the pigment composition, which led to differences in shade, but not in translucency [5]. More recently, a different strategy has been adopted, in which different compositions and microstructures can be found in the same material (e.max ZirCAD Multi, Ivoclar Vivadent). According to the manufacturer, this material has four distinct layers: the incisal one-third (enamel) contains a 5 mol.% yttria partially stabilized zirconia (5Y-PSZ); the body layer (dentin), which is the gingival counterpart, has a 4 mol.% partially stabilized zirconia (4Y-PSZ); and the composition of the two intermediate layers that integrate the enamel and body layers is unknown. As a result, the unique property of a gradual progression of shade and translucency permits the use of this material for a broad spectrum of clinical indications, including anterior veneers with high esthetic demands.

Nevertheless, the effect of the composition and microstructure gradients on the mechanical behavior of these new multi-layered materials has not been investigated. The literature shows that 4Y-PSZ and 5Y-PSZ have lower fracture strength and toughness than the conventional 3Y-TZP, due mainly to the reduced ability of transformation toughening associated with a decrease in tetragonal zirconia content [3, 6, 8, 9]. Additionally, as 5Y-PSZ has higher cubic content than 4Y-PSZ, their mechanical properties also differ from each other [5, 7, 10].

Clinically, restorations are exposed to a hostile humid environment with varying pH levels and temperatures. Chewing and parafunctional habits can induce both axial and off-axial forces to the restoration [5, 11-13]. During the mandibular movements, the antagonist slides

over the restoration surface across different layers of the multi-layered zirconia, where its composition, microstructure and wear behavior is still unclear. The wear produced by the contact with the antagonist is classified as attrition (two-body wear) and could result in surface damage, with crack initiation and propagation, and loss of material, leading to failures [2, 14-20]. Although zirconia-based materials are more wear resistant than the tooth enamel, extensive prosthetic rehabilitation has become very common in dentistry and other wear-resistant restorative materials may also be found as the antagonist [21-23].

Literature on the wear behavior of the third- and fourth-generations, cubic-containing zirconia is limited; furthermore, none of the studies focused on the multi-layered material with compositional and microstructural gradients [24-26]. In addition, only a few clinical reports on the multi-layered zirconia restorations are available [27]. Therefore, it is important to understand the structure and wear behavior of the new multilayer zirconia in order to support its clinical indications. Accordingly, the objectives of this study are to characterize the composition, microstructure and wear properties of a multilayer translucent zirconia dental ceramic (MULTI, IPS e.max ZirCAD Multi, Ivoclar Vivadent) in relation to its multi-transition zones as well as to compare its properties with a conventional monolithic 3Y-TZP ceramic (IPS e.max ZirCAD LT, Ivoclar Vivadent).

2. Materials and Methods

A multilayer translucent zirconia ceramic (MULTI, IPS e.max ZirCAD Multi, Ivoclar Vivadent) and a conventional 3Y-TZP (3Y, IPS e.max ZirCAD LT, Ivoclar Vivadent) control were investigated. Material description can be found in Table 1.

2.1 Composition and Microstructure

2.1.1 Zirconia phase quantification—MULTI blocks were cut into three parts to obtain samples of each layer using a low speed diamond saw (Isomet 1000, Buehler, USA). For enamel and dentin layers, specimens were cut from the top and bottom of the block. For transition layers, the middle part of the block was used; the surface near the enamel layer was designated as transition zone 1 (T1) and the surface near the dentin layer, transition zone 2 (T2). The material was sectioned according to a careful microscopic analysis of the location of each layer (layer thickness). A specimen from 3Y control group was also obtained by cutting the ceramic block. All specimens were ground using silicon carbide paper with 320-grit and 800-grit in order to obtain flat surfaces. The same sintering protocol (1500 °C for 2 h) was performed for both materials, following the manufacturer instructions.

In order to identify the crystalline phase fractions, specimens were analyzed by X-ray diffraction (XRD, X'Pert3 Powder, PANalytical, Netherlands). Scanning conditions were set as follows: the tube voltage 40 kV, tube current 45 mA, with CuKα radiation (λ = 1.5418 Å) using a step-scanning technique with a fixed step size of 0.01° and a rate of 0.3 seconds/step, over a 2θ range between 20° and 80°. A full-profile fitting technique was used to precisely calculate the phase fractions of each material by the Rietveld refinement method implemented in the HighScore Plus software [28]. The diffractograms were used to quantify phases of zirconia by focusing on tetragonal (002 and 200) and cubic (111) peaks around 2θ = 35°.

2.1.2 Microstructure analysis—To analyze the microstructure and measure the grain size, specimens from each layer of MULTI and 3Y were produced ($n = 2$), as described above for the X-ray analysis. After sintering, one surface of the zirconia specimen was further polished to 1 μm finish using a polishing machine (Ecomet Polisher, Buehler, USA) to obtain a final dimension of 12.8 x 12.8 x 1 mm. Specimens were then thermally etched at 1150 °C for 20 min with heating and cooling rates of 10 °C per min.

After cooling, the specimens were ultrasonically cleaned in ethanol for 5 min. Prior to imaging in a Field Emission Scanning Electron Microscopy (FE-SEM, Merlin, Carl Zeiss), specimens were coated with a nanometric layer of iridium. The grain size was measured on SEM micrographs using the linear intercept technique [29]. The average grain size (D) was obtained using $= 1.56\frac{C}{MN}$, where C is the total length of test line used, N the number of intercepts and M the magnification of the photomicrograph. The proportional constant, 1.56, is essential for random slices through a model system consisting of space-filling tetrakaidekahedral shaped grains with a lognormal size distribution.

2.2 Wear Characteristics

2.2.1 Specimen preparation—MULTI and 3Y ceramics were evaluated in the oral wear simulator ($n = 12$). Specimens of MULTI and 3Y were produced and polished to 1 μm finish, as described for the microstructure analysis.

Zirconia specimens were cemented to a dentin analog substrate (G10, glass-fiber reinforced epoxy resin rods, Acculam, USA) with a dual-cure resin cement. G10 cementation surface was acid-etched with 5% hydrofluoric acid (Ceramic Etching Gel, Ivoclar Vivadent) for 2 min, while the ceramic surface was air-abraded with 50 μm alumina particles at 3 bars pressure for 20 s. After cleaning the G10 and ceramic surfaces, a bonding agent (Monobond Plus, Ivoclar Vivadent) was applied for 60 s and air dried. Ceramic specimens were then cemented to the dentin analog using Multilink Automix dual-cure resin cement (Ivoclar Vivadent). A 9.8 N load was kept over the ceramic specimen for 5 min to ensure a uniform cement layer and specimens were light cured for 30 s on each side using a dental curing light (Bluephase Style, Ivoclar Vivadent). The bonded specimens were kept in distilled water at 37 °C for 3 days in an incubator (Isotemp Incubator, Fisher Scientific, USA) prior to testing in the oral wear simulator.

2.2.2 Wear tests—A 4-chamber Oregon Health Science University (OHSU) oral wear simulator (Proto-tech, USA) was used in this study. The test was performed as follows: (1) a 30 N vertical load was applied through a zirconia spherical antagonist ($r = 3.15$ mm) to the ceramic surface, (2) the antagonist advances across the specimen surface in a 5-mm horizontal path, (3) the load level decreases at the end of the path as the antagonist lifts out of contact while returning to its original position, to begin a new cycle.

Careful examinations of sintered MULTI specimens by optical microscopy revealed that the thicknesses of the enamel, T1, T2, and dentin layers are 2.56, 1.15, 1.40, 7.68 mm, respectively (Fig. 1). To ensure the antagonist has traversed all four layers, the 5-mm cyclic sliding action began with positioning the antagonist 2 mm away from the surface of the

enamel layer (5Y), sliding across the 2 transition layers (T1 and T2), and ending in the dentin layer (4Y) approximately 1.89 mm away from the T2/dentin interface (Fig. 1).

Tests were conducted for a total of 500,000 sliding cycles at a frequency of 1.5 Hz in distilled water. The test was interrupted at 10,000, 50,000, 100,000, 200,000, 300,000, 400,000 and 500,000 cycles to obtain images of the wear scar on the specimen surface using an optical microscope (Leica MZAPO Stereo microscope, Leica Microsystems).

2.2.3 Wear analysis—The dimension (length: l and width: w) of the wear scars was measured after N = 10,000, 50,000, 100,000, 200,000, 300,000, 400,000 and 500,000 cycles with Adobe Photoshop (Photoshop CC) using optical microscopy images.

To measure the volume loss and maximum wear depth after 500,000 cycles, high-resolution (10 μm) tomography scanning of the wear crater was performed on a Laser Scanner (SD Mechatronic Laser Scanner LAS-20). The collected data were analyzed using a 3D reconstruction software (3D-System Geomatic Wrap). The original topography of the zirconia surface was reconstructed by means of mesh editing, based on the intact edges of the specimen. The two models—the original surface and the wear surface—were superimposed and the maximum distance from the scar to the original surface was used to measure the maximum wear depth. The two models were then subtracted to create a third model that was used to calculate the scar volume.

The surface and sub-surface damage introduced to the specimens by the oral wear simulation was investigated using optical and scanning electron microscopy (Zeiss EVO 50 SEM, USA). Surface damage was analyzed by mapping the wear scar. Sub-surface damage was investigated using a sectioning technique [30, 31]. Specimens were embedded in epoxy resin and sectioned across the centerline of the wear scar along the sliding direction using a low speed saw (Isomet 5000, Buehler). The cross-sections were polished to 1-μm finish prior to microscopic analysis.

The two-way ANOVA (factors: material and number of cycles) was used to analyze the dimensions (length and width) of the wear scar ($\alpha = 0.05$). Volume loss (mm^3) and maximum wear depth (mm) data of MULTI versus 3Y were analyzed with the Student´s t-test ($\alpha = 0.05$).

3. Results

3.1 Composition and Microstructure

3.1.1 Zirconia phase quantification—XRD patterns, between 20° and 80°, for each layer of MULTI and for 3Y control are shown in Figure 2a. No monoclinic phase was detected in any of the investigated materials. Rietveld analysis revealed that the enamel layer had the highest amount of cubic content, followed by T1, T2 and dentin layers (Table 1). 3Y had the lowest fraction of cubic zirconia.

3.1.2 Microstructural analysis—FE-SEM images of each layer of MULTI and the 3Y control group are shown in Figures 2b-f. No porosity was found in all materials. The largest

average grain size was observed from the enamel layer followed by T1, T2 and dentin layer, as shown in Table 1. 3Y showed the smallest grain size.

3.2 Wear Data

The mean length (l) and width (w) of the scar measured after different number of cycles (N) for each ceramic is presented in Figure 3. Error bars represent standard error values. To provide perspective on the wear progression as a function of sliding distance (L), the corresponding sliding distance to a given number of contact cycles is also given in the secondary x-axis. For the scar length, the factor material ($p = 0.537$) and the interaction between factors ($p = 0.991$) were not significant. Only the factor number of cycles was significant ($p < 0.001$), meaning that the length of the scar increased with the number of cycles or sliding distance. For the scar width, the factor material ($p = 0.192$) and the interaction between factors ($p = 0.984$) were not significant, while the factor number of cycles was significant ($p < 0.001$).

Nonetheless, two distinctive regions were apparent for both materials: an initial run-in stage with higher wear rates and a steady-state stage with lower slopes of the curves after 5×10^4 sliding cycles. To confirm our observation, Figure 4 plots the measured wear scar length versus width, for scars at the end of each pre-determined sliding cycles/distance in Figure 3. Filled symbols represent steady-state data sets, while open symbols run-in data sets. Error bars correspond to standard error values. The solid line represents the steady-state wear rate. Despite relatively large error bars, the initial data points, corresponding to $N = 10^4$ sliding cycles, clearly fall below the steady-state line, indicating a run-in phase.

It is important to note that significant statistical differences were found between MULTI and 3Y groups for volume loss ($p = 0.007$) and for maximum wear depth ($p = 0.001$). MULTI showed greater volume loss and wear depth than 3Y after 500,000 sliding cycles (Table 2).

During the oral wear simulation, replicas of the zirconia antagonists were produced for the different number of cycles evaluated. These replicas and the zirconia antagonists ($N =$ 500,000 cycles) were analyzed using an optical microscope. Only very small and shallow wear scars (not measurable) were found.

Figures 5, 6 and 7 show representative images of surface damage introduced in both ceramics after 500,000 cycles of oral wear simulation. 3Y wear surface presented a high density of partial cone cracks distributed throughout the entire wear track (Figs. 5-7a). But for MULTI, cracks were only apparent close to the endpoint of the wear scar. Grain dislodgment was, however, observed in the wear crater across all four layers (Figs. 6-7b). In both materials, cracks also formed towards the end of the wear crater due predominantly to the intensified compressive stress at the leading edge of the moving antagonist [32, 33].

Sub-surface damage sustained in both materials following 500,000 sliding cycles is shown in Figure 8. Images were obtained using the secondary electron emission mode on the cross-sections of the wear scars. A more severe wear pattern was observed in the MULTI material, along with the formation and propagation of lateral cracks that lead to material loss, resulting in a rougher surface than 3Y.

Surface and sub-surface analysis of the scar showed that the wear pattern across all four layers of the MULTI material was similar (Figs. 5-8). These results indicate that the presence of transition layers had no effect on the wear behavior of multi-layered zirconia.

4. Discussion

The present study investigated how the composition and microstructure of the different layers of a translucent multi-layered zirconia affect its wear behavior in comparison to a conventional 3Y-TZP. Microstructure analysis and zirconia phase quantification showed different grain size and phase content for the different layers of MULTI material. The grain size and cubic content reduce gradually from the enamel to the dentin layer. The enamel layer and its adjacent transition zone 1 have a higher cubic content (> 60 wt.%) and average grain size (> 1.7 μm) than those of transition zone 2 and the dentin layer. These findings are in accordance with the information provided by the manufacturer, which stated that the enamel layer is composed of 5Y-PSZ and the dentin layer is 4Y-PSZ. On the contrary, the 3Y control showed a smaller grain size with less than 15 wt.% cubic content.

When the wear scar width and length were measured after different numbers of sliding cycles, there were no differences between MULTI and 3Y. Yet, when the scar depth and volume after 500,000 cycles were analyzed, MULTI showed higher maximum wear depth and volume loss than 3Y. The width and the length of the wear scar are two-dimensional measurements and could mislead the study conclusions, especially when the differences between the wear of the materials is small. Maximum wear depth combined with volume loss can provide a three-dimensional view of the wear scar and a better understanding of the wear process [14]. In the present study, the scar dimension was measured aiming to evaluate the wear progress over time, which was similar among materials. A significant increase in the dimension of the wear scar was observed in the initial stage (up to 50,000 cycles) and later the wear progression reaches a steady state. Clinically, it is also expected that the wear rate would decrease with time due to intra-oral wear processes, including occlusal self-adjustments [34, 35].

Two regimes of sliding wear can be identified in the ceramic materials: mild wear and severe wear [16, 17, 24, 25, 36]. Microplasticity is the dominant wear mechanism for mild wear, whereas micro-cracking is a dominant factor causing severe wear [36, 37]. Surface and sub-surface damage analysis indicated that 3Y and MULTI underwent severe wear, as cracks and fractures were observed in both materials. Nevertheless, distinct wear patterns were observed for the ceramics, justifying the differences in the maximum wear depth and volume loss. For 3Y, a uniform crack distribution along the entire wear track was found, as seen in Figure 5. For MULTI, cracks were mainly observed towards the end of the wear track in the dentin layer, whereas cumulative damage led to the dislodgment of clusters of zirconia particles in all four layers (Fig. 6). Sub-surface analysis revealed extensive lateral cracking that initiated beneath the contact surface of MULTI, propagated in the direction parallel to the surface then eventually intersected with the surface, resulting in localized material spalling and thus increased the surface roughness (Fig. 8). Moreover, as a result of surface spallation, MULTI could be subjected to a three-body abrasive wear, leading to more aggressive wear conditions over time.

These distinct wear patterns can be attributed to the differences in the microstructure, composition, mechanical and physical properties of the materials. High tensile stresses are induced in the materials' surface during repeated sliding contact, resulting in a mechanism called fatigue wear. Fatigue propagated cracks are further affected by hydraulic pumping and slow crack growth (SCG) in a humid environment [32, 38]. 3Y is more resistant to crack initiation and propagation than 4Y-PSZ and 5Y-PSZ, which are the constituents of the MULTI material (Table 1) [3, 6, 8]. Therefore, after 500,000 cycles of oral wear simulation, 3Y surface pattern suggests an earlier stage of fatigue wear, while MULTI reached a more advanced stage, showing a higher amount of material spalling and sub-surface cracks.

Previous studies have investigated the third-generation, high cubic-content zirconia and reported similar wear behavior to conventional 3Y-TZP [24, 25]. Yet, in these studies mild wear conditions were found, in which grain pullout was the principal wear mechanism and no micro-cracks and fractures were identified. The wear mechanisms are dependent on the testing conditions (i.e. load, frequency, lubricant, antagonist, time) and different methods are used in the investigations [14-16, 24, 25]. In the present study, micro-cracks and fractures that are indicative of severe wear were observed in both ceramics. Additionally, the method used to quantify wear varies and zirconia-based ceramics present very shallow scars, which usually impairs accurate measurement of volume loss [14, 15, 24]. In our methodology, quantitative wear measurements were performed by reconstructing the original three-dimensional surface of the specimens rather than scanning the surface before and after the wear test in order to minimize errors related to data acquisition.

The oral wear simulation was performed in distilled water to simulate the oral environment. The load and frequency were also defined according to clinical parameters [5, 11, 12]. A 3Y-TZP zirconia antagonist was chosen for the test aiming to quantify wear against a hard indenter, being a harsher condition than wear against the tooth, which could be a limitation. Yet, monolithic restorations of zirconia and other ceramics can be found as an antagonist in oral rehabilitation treatments. The wear simulator performs a longer horizontal excursion than the sliding path observed during a physiological chewing motion, typically being 0.9 – 1.2 mm on the anterior teeth. [39]. Thus, the actual volume loss in a clinical setting would be 4 to 6 times less than that in the simulator. We chose a 'long' 5-mm path so that the antagonist would slide cross all four layers of the MULTI material, allowing a careful characterization of its wear behavior.

Clinically, restorations are subjected to a less aggressive environment. Nevertheless, it is important to notice that, although the quantitative wear analysis only indicated small differences between materials, the wear pattern suggests that MULTI is more susceptible to fatigue wear than 3Y, which could affect its clinical performance. Yet, the wear pattern across all four layers of the MULTI material was similar, meaning that the composition and microstructure gradients resulted in a homogeneous behavior, supporting its clinical indications.

5. Conclusions

The wear pattern in multi-layered zirconia was more rugged than the control (3Y-TZP). This is due mainly to the formation of extensive subsurface lateral cracks in multi-layered zirconia, which ultimately result in localized material spalling, leading to a greater amount of volume loss and wear depth.

Although the grain size and cubic content of the multilayer translucent zirconia reduced gradually from the enamel to the dentin layer, the presence of different layers had no effect on its wear behavior.

Acknowledgements

This work was supported by the U.S. National Institutes of Health / National Institute of Dental and Craniofacial Research (grant numbers R01DE026279 and R01DE026772) and by FAPERGS and CAPES Brazilian agencies (grant number 19/2551-0000677-2)

References

1. Zhang Y, Kelly JR. Dental Ceramics for Restoration and Metal Veneering. Dental clinics of North America 2017;61(4):797–819. [PubMed: 28886769]
2. Stawarczyk B, Frevert K, Ender A, Roos M, Sener B, Wimmer T. Comparison of four monolithic zirconia materials with conventional ones: Contrast ratio, grain size, four-point flexural strength and two-body wear. J Mech Behav Biomed Mater 2016;59:128–138. [PubMed: 26751707]
3. Camposilvan E, Leone R, Gremillard L, Sorrentino R, Zarone F, Ferrari M, et al. Aging resistance, mechanical properties and translucency of different yttria-stabilized zirconia ceramics for monolithic dental crown applications. Dent Mater 2018;34(6):879–890. [PubMed: 29598882]
4. Zhang Y, Lawn BR. Novel Zirconia Materials in Dentistry. J Dent Res 2018;97(2):140–147. [PubMed: 29035694]
5. Kolakarnprasert N, Kaizer MR, Kim DK, Zhang Y. New multi-layered zirconias: Composition,microstructure and translucency. Dent Mater 2019;35:797–806. [PubMed: 30853208]
6. Mao L, Kaizer MR, Zhao M, Guo B, Song YF, Zhang Y. Graded ultra-translucent zirconia (5y-psz) for strength and functionalities. Journal of Dental Research 2018.
7. Kaizer MR, Kolakarnprasert N, Rodrigues C, Chai H, Zhang Y. Probing the interfacial strength of novel multi-layer zirconias. Dent Mater 2020;36(1):60–67. [PubMed: 31727444]
8. Zhang F, Inokoshi M, Batuk M, Hadermann J, Naert I, Van Meerbeek B, et al. Strength, toughness and aging stability of highly-translucent Y-TZP ceramics for dental restorations. Dent Mater 2016;32(12):e327–e337. [PubMed: 27697332]
9. Borba M, de Araujo MD, Fukushima KA, Yoshimura HN, Cesar PF, Griggs JA, et al. Effect of the microstructure on the lifetime of dental ceramics. Dent Mater 2011;27(7):710–721. [PubMed: 21536324]
10. Yan J, Kaizer MR, Zhang Y. Load-bearing capacity of lithium disilicate and ultra-translucent zirconias. Journal of the mechanical behavior of biomedical materials 2018.
11. Zhang Y, Sailer I, Lawn BR. Fatigue of dental ceramics. J Dent 2013;41(12):1135–1147. [PubMed: 24135295]
12. Kelly JR. Clinically relevant approach to failure testing of all-ceramic restorations. J Prosthet Dent 1999;81(6):652–661. [PubMed: 10347352]
13. Kim JH, Kim JW, Myoung SW, Pines M, Zhang Y. Damage maps for layered ceramics under simulated mastication. Journal of dental research 2008;87(7):671–675. [PubMed: 18573989]
14. Heintze SD. How to qualify and validate wear simulation devices and methods. Dent Mater 2006;22(8):712–734. [PubMed: 16574212]

15. Kaizer MR, Bano S, Borba M, Garg V, dos Santos MBF, Zhang Y. Wear behavior of graded glass/zirconia crowns and their antagonists. JDR 2019;98(4):437–442. [PubMed: 30744472]
16. Kaizer MR, Gierthmuehlen PC, Dos Santos MB, Cava SS, Zhang Y. Speed sintering translucent zirconia for chairside one-visit dental restorations: Optical, mechanical, and wear characteristics. Ceram Int 2017;43(14):10999–11005. [PubMed: 29097830]
17. Kaizer MR, Moraes RR, Cava SS, Zhang Y. The progressive wear and abrasiveness of novel graded glass/zirconia materials relative to their dental ceramic counterparts. Dent Mater 2019;35(5):763–771. [PubMed: 30827797]
18. Wendler M, Kaizer MR, Belli R, Lohbauer U, Zhang Y. Sliding contact wear and subsurface damage of CAD/CAM materials against zirconia. Dent Mater 2020;36(3):387–401. [PubMed: 32007314]
19. Mair LH. Wear in dentistry--current terminology. Journal of dentistry 1992;20(3):140–144. [PubMed: 1624617]
20. Heintze SD, Zellweger G, Grunert I, Munoz-Viveros CA, Hagenbuch K. Laboratory methods for evaluating the wear of denture teeth and their correlation with clinical results. Dent Mater 2012;28(3):261–272. [PubMed: 22104731]
21. Cardelli P, Manobianco FP, Serafini N, Murmura G, Beuer F. Full-Arch, Implant-Supported Monolithic Zirconia Rehabilitations: Pilot Clinical Evaluation of Wear Against Natural or Composite Teeth. J Prosthodont 2016;25(8):629–633. [PubMed: 26436677]
22. Hansen TL, Schriwer C, Oilo M, Gjengedal H. Monolithic zirconia crowns in the aesthetic zone in heavy grinders with severe tooth wear - An observational case-series. J Dent 2018;72:14–20. [PubMed: 29452242]
23. Esquivel J, Lawson NC, Kee E, Bruggers K, Blatz MB. Wear of resin teeth opposing zirconia. The Journal of prosthetic dentistry 2020.
24. Zhang F, Spies BC, Vleugels J, Reveron H, Wesemann C, Muller WD, et al. High-translucent yttria-stabilized zirconia ceramics are wear-resistant and antagonist-friendly. Dent Mater 2019;35(12):1776–1790. [PubMed: 31727445]
25. Borrero-Lopez O, Guiberteau F, Zhang Y, Lawn BR. Wear of ceramic-based dental materials. J Mech Behav Biomed Mater 2019;92:144–151. [PubMed: 30685728]
26. Kwon SJ, Lawson NC, McLaren EE, Nejat AH, Burgess JO. Comparison of the mechanical properties of translucent zirconia and lithium disilicate. The Journal of prosthetic dentistry 2018;120(1):132–137. [PubMed: 29310875]
27. Sesemann MR, Culp L, Swann L. Restoration of Extremely Dark Tetracycline-Stained Teeth with Monolithic Gradient Zirconia. Journal of Cosmetic Dentistry 2018;34(2):28–38.
28. Lutterotti L, Scardi P. Simultaneous structure and size-strain refinement by the Rietveld method. Journal of Applied Crystallography 1990;23(4):246–252
29. Wurst JC, Nelson JA. Lineal Intercept Technique for Measuring Grain Size in Two-Phase Polycrystalline Ceramics. Journal of the American Ceramic Society 1972;55(2):109–109.
30. Kim JW, Kim JH, Janal MN, Zhang Y. Damage maps of veneered zirconia under simulated mastication. Journal of dental research 2008;87(12):1127–1132. [PubMed: 19029080]
31. Stappert CF, Baldassarri M, Zhang Y, Stappert D, Thompson VP. Contact fatigue response of porcelain-veneered alumina model systems. Journal of biomedical materials research. Part B, Applied biomaterials 2012;100(2):508–515.
32. Kim JW, Kim JH, Thompson VP, Zhang Y. Sliding contact fatigue damage in layered ceramic structures. J Dent Res 2007;86(11):1046–1050. [PubMed: 17959894]
33. Zhang Y, Kim J-W, Kim J-H, Lawn BR. Fatigue Damage in Ceramic Coatings From Cyclic Contact Loading With a Tangential Component. Journal of the American Ceramic Society 2008;91(1):198–202.
34. Lambrechts P, Braem M, Vuylsteke-Wauters M, Vanherle G. Quantitative in vivo wear of human enamel. Journal of dental research 1989;68(12):1752–1754. [PubMed: 2600255]
35. Stober T, Bermejo JL, Schwindling FS, Schmitter M. Clinical assessment of enamel wear caused by monolithic zirconia crowns. J Oral Rehabil 2016;43(8):621–629. [PubMed: 27198539]
36. Liu H, Xue Q. Wear mechanisms of zirconia/steel reciprocating sliding couple under water lubrication. Wear 1996;201:51–57.

37. Ren L, Zhang Y. Sliding contact fracture of dental ceramics: Principles and validation. Acta Biomater 2014;10(7):3243–3253. [PubMed: 24632538]

38. Zhang Y, Song JK, Lawn BR. Deep-penetrating conical cracks in brittle layers from hydraulic cyclic contact. J Biomed Mater Res B Appl Biomater 2005;73(1):186–193. [PubMed: 15672403]

39. Rilo B, Fernandez J, Da Silva L, Martinez Insua A, Santana U. Frontal-plane lateral border movements and chewing cycle characteristics. Journal of oral rehabilitation 2001;28(10):930–936. [PubMed: 11737564]

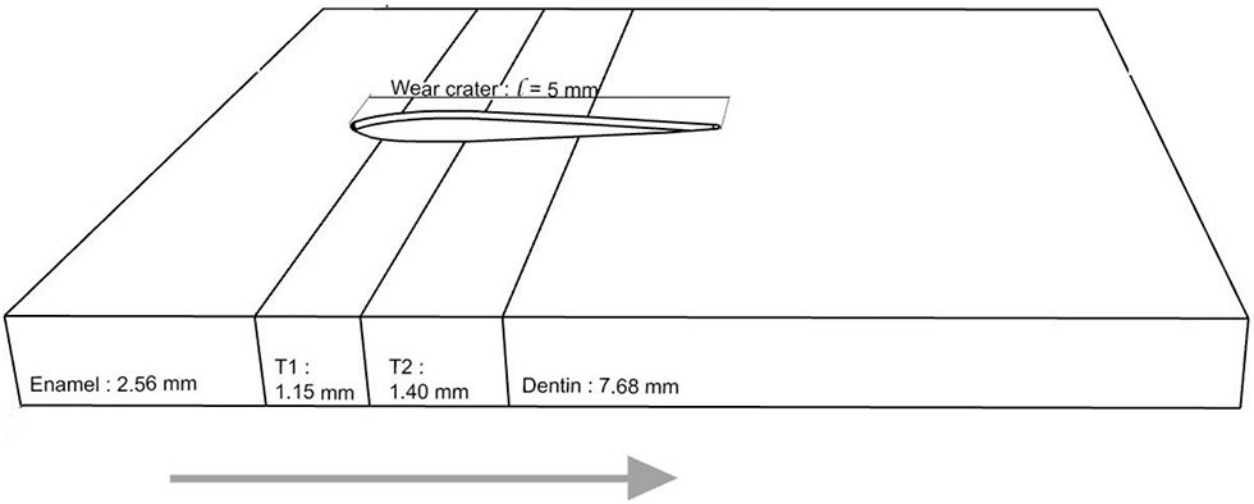

Figure 1.

Schematic of multilayer zirconia specimens prepared for the current study, showing the thickness of individual layers and the relative position of the sliding trajectory. Arrow indicates the antagonist sliding direction (from left to right).

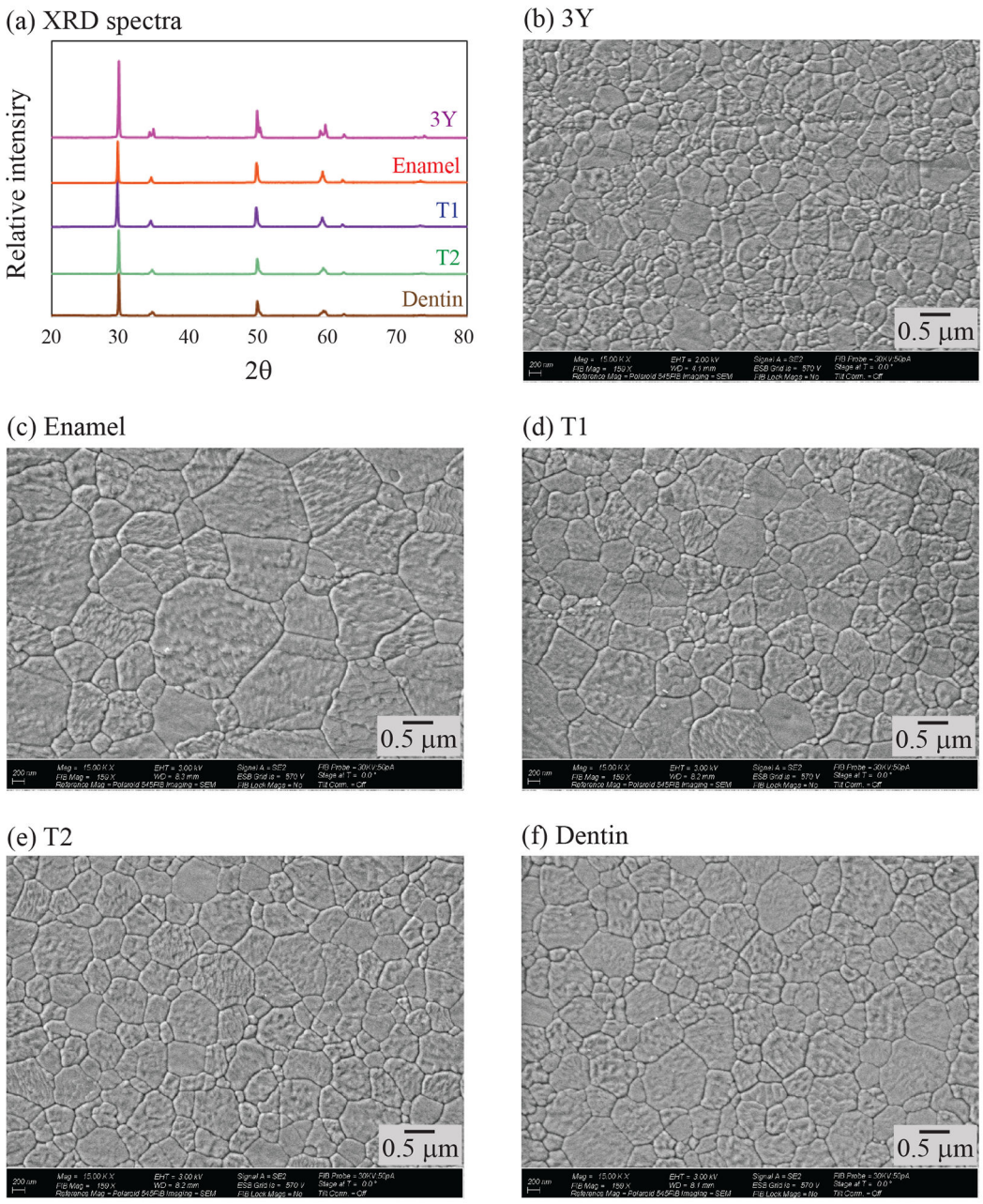

Figure 2.

(a) XRD pattern for each layer of MULTI (enamel, T1, T2 and dentin), and for the 3Y control. Representative FE-SEM images of the investigated materials: (b) 3Y, (c) enamel layer, (d) T1, (e) T2, (f) dentin layer.

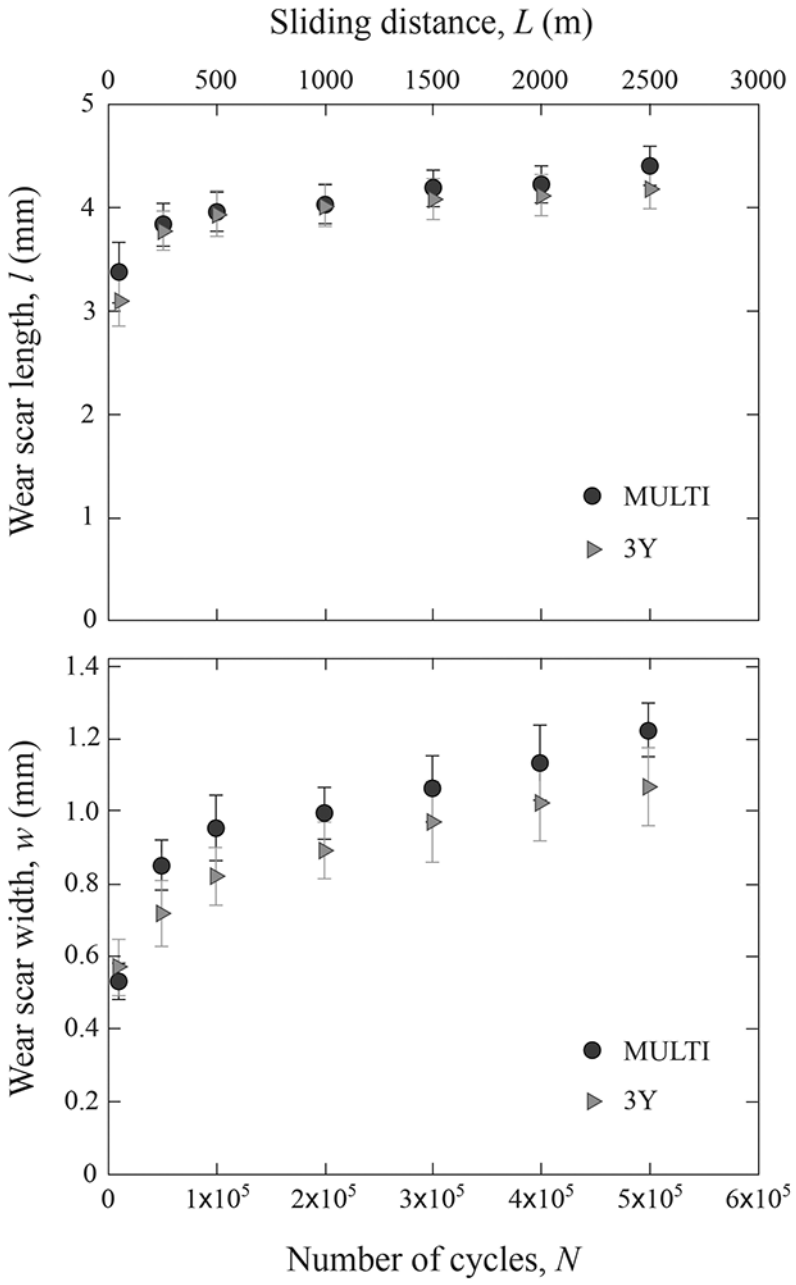

Figure 3.

Graphs showing the mean scar length *l* (a) and width *w* (b) of MULTI and 3Y after various numbers of cycles (*N*) and sliding distances (*L*). Data are presented as the mean and standard error of the mean.

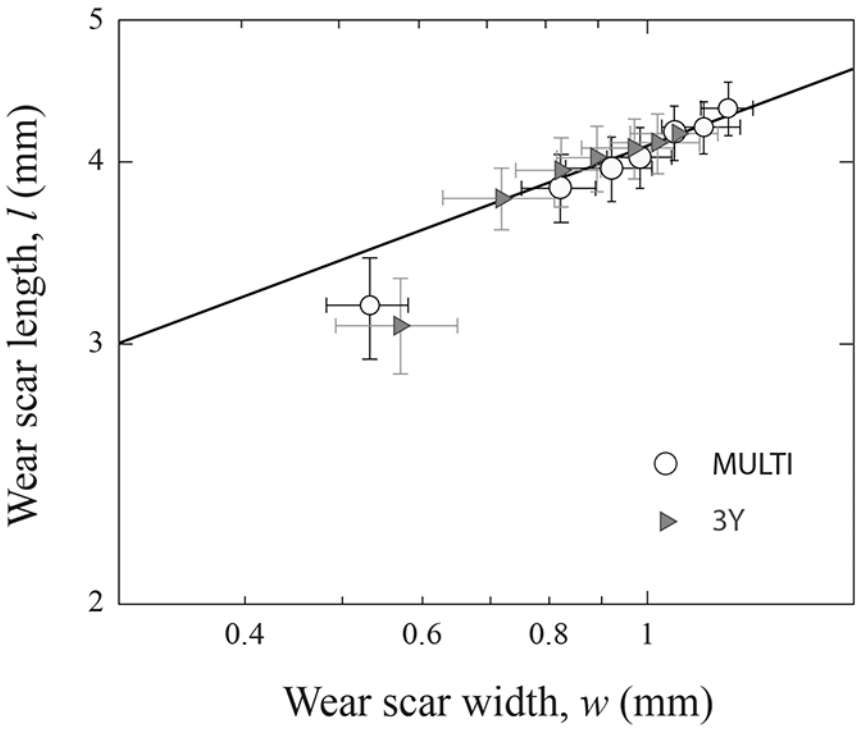

Figure 4.

Plot of wear scar length *l* versus width *w*. Measurements were made following each predetermined sliding cycles in Fig. 3. Data are presented in mean and standard error of the mean. Solid line is simply a best fit through the steady state data sets.

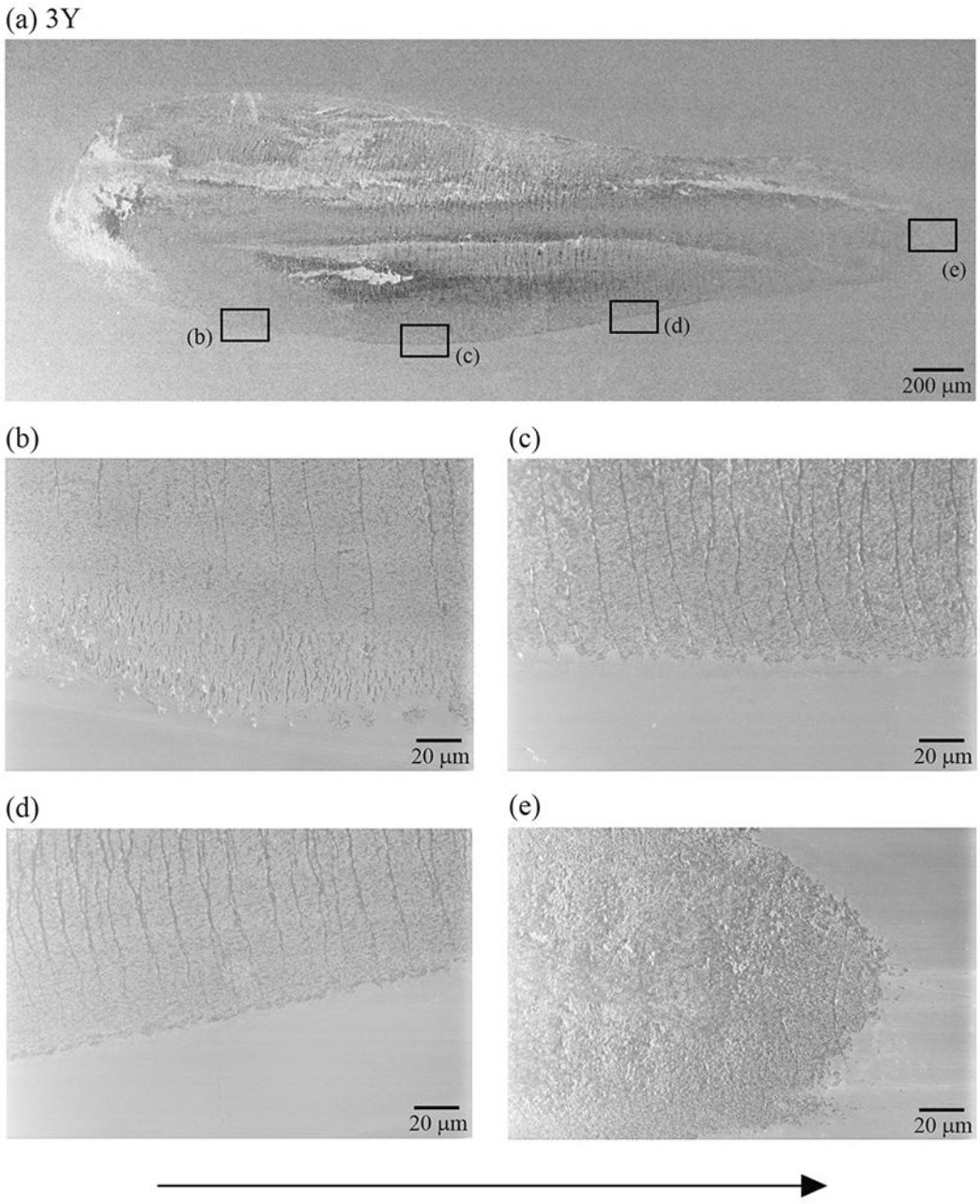

Figure 5.

(a) The representative SEM image of the wear scar of a 3Y specimen after 500,000 cycles of oral wear simulation. Images (b) to (e) are higher magnification views of the 3Y wear scar showing that cracks are distributed throughout the entire extension of the scar. The sliding direction of the antagonist is from left to right (black arrow).

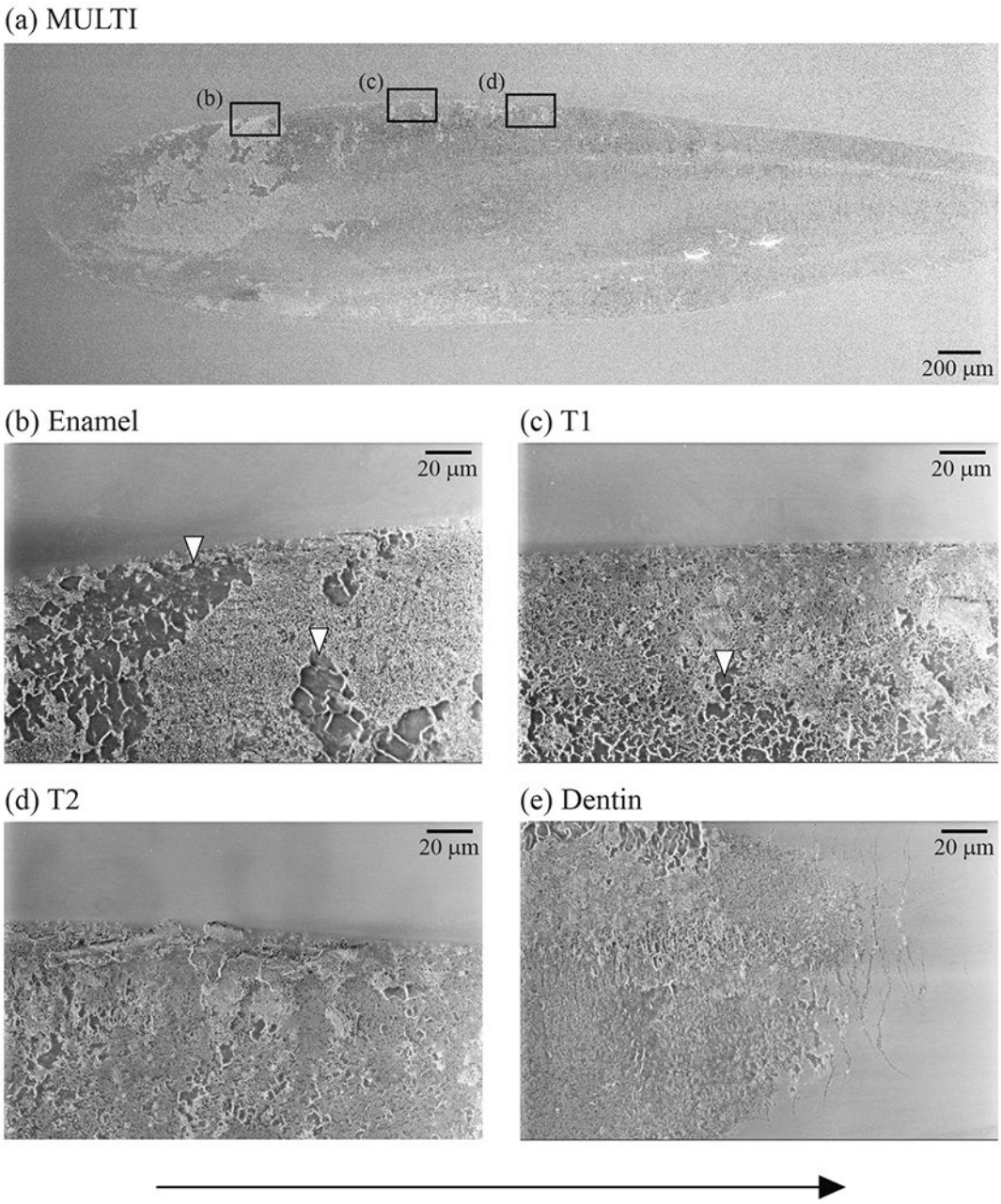

Figure 6.

(a) The representative SEM image of the wear scar of a MULTI specimen after 500,000 cycles of oral-wear simulation. Images (b) to (e) are higher magnification views of the wear surface of each layer of MULTI material. White arrows point to areas of grains dislodgement. Cracks are located ahead of the wear scar, as shown in image (e). The sliding direction of the antagonist is from left to right (black arrow).

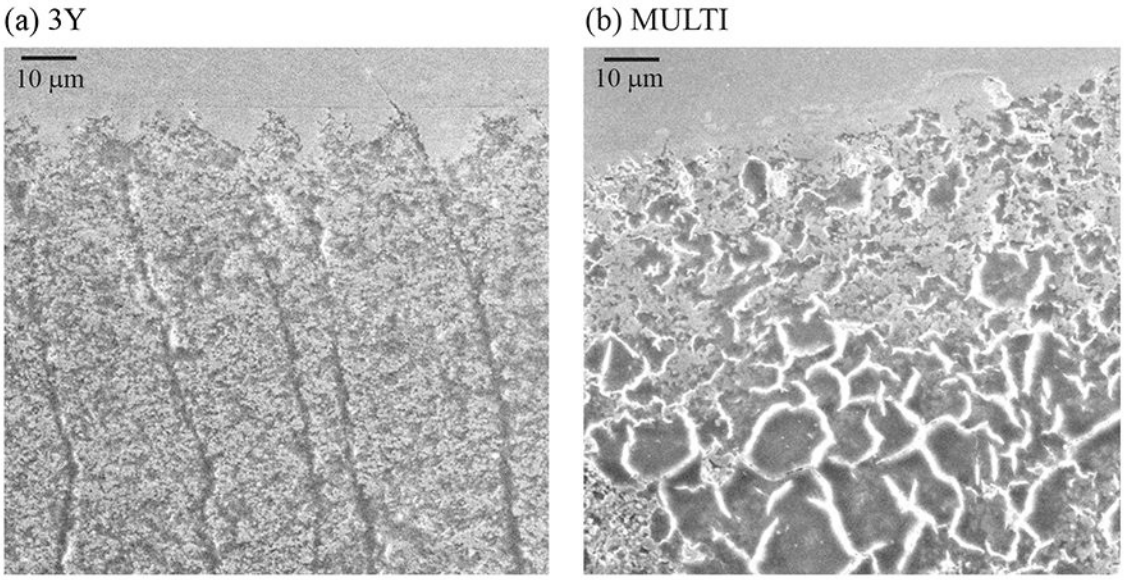

Figure 7.

SEM images of the wear scar damage of 3Y (a) and MULTI (b) specimens after 500,000 cycles of oral-wear simulation. The sliding direction of the antagonist is from left to right.

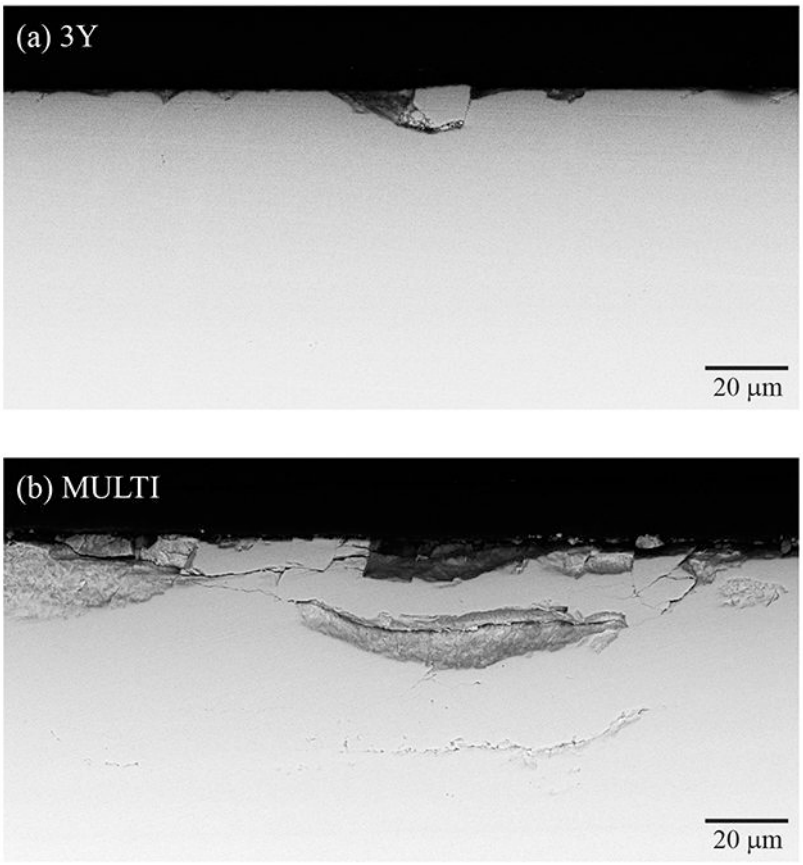

Figure 8.
Cross-sectional SEM images of the sub-surface damage introduced in 3Y (a) and MULTI (b) specimens after 500,000 cycles. The sliding direction of the antagonist is from left to right (black arrow).

Table 1.

Description of materials used in the study.

Legend	Material	Mean Grain Size (standard-deviation)[b]	Cubic Content[b]	Mean Flexural Strength (standard-deviation)[b]	Fracture Toughness[a]	Mean Translucency Parameter (standard-deviation)[b]	Clinical Indication[a]
MULTI	IPS e.max ZirCAD Multi (Ivoclar Vivadent)	Enamel layer: 1.87 (0.35) μm T1: 1.72 (0.32) μm T2: 1.40 (0.15) μm Dentin Layer: 1.12 (0.21) μm	Enamel layer: 80 wt.% T1: 64 wt.% T2: 49 wt.% Dentin Layer: 46 wt.%	Enamel layer: 387 (60) MPa Dentin layer: 744 (104) MPa	3.6 MPa·m$^{1/2}$	Enamel layer 36.7 (1.7) Dentin layer 29.0 (0.7)	Full-contour crowns, full-contour 3-unit bridges, implant-supported superstructures
3Y	IPS e.max ZirCAD LT (Ivoclar Vivadent)	1.08 (0.23) μm	15 wt.%	851 (97) MPa	5.0 MPa·m$^{1/2}$	26.3 (0.0)	Full-contour crowns, full-contour 3- and 4-unit to multi-unit bridges, frameworks, implant-supported superstructure

[a] Information from manufacturer's data sheets.

[b] Measured in the author's laboratory.

Table 2:

Mean (standard error) values of volume loss (mm^3) and maximum wear depth (mm) after 500,000 cycles for MULTI and 3Y.

Group	Volume (mm^3)	Depth (mm)
MULTI	0.08 (0.007) [a]	0.04 (0.003) [a]
3Y	0.04 (0.007) [b]	0.03 (0.004) [b]

*Mean values followed by different letters in the same column are statistically different ($p < 0.05$).